

## Experimental analysis to identify colored noises in electrical systems

### Análisis experimental para clasificar ruidos de colores en sistemas eléctricos

HERNÁNDEZ-SANTIAGO, Joaquín†, ALEJANDRO-CRISANTOS, Carlos, ESCOBEDO-TRUJILLO, Beatris Adriana\*, GARRIDO-MELÉNDEZ, Javier

*Universidad Veracruzana, Facultad de Ingeniería, Avenida Universidad km 7.5, Colonia Santa Isabel, C.P. 96535, Coatzacoalcos, Veracruz 96535, México.*

ID 1<sup>st</sup> Author: Joaquín, Hernández-Santiago / ORC ID: 0000-0003-1031-1016

ID 1<sup>st</sup> Co-author: Carlos, Alejandro-Crisantos

ID 2<sup>nd</sup> Co-author: Beatris, Adriana, Escobedo-Trujillo / ORC ID: 0000-0002-8937-3019, Scopus ID: 54417142300, CVU CONACYT ID: 173174

ID 3<sup>ed</sup> Coautor: Javier, Garrido-Meléndez / ORC ID: 0000-0001-9143-408X, - Researcher ID Thomson: C-9373-2018

DOI: 10.35429/JSI.2022.19.6.31.41

Received March 14, 2022; Accepted June 29, 2022

#### Abstract

The main objective of this paper is to identify the several types of color noise existing in electrical systems, a methodology is proposed for the identification of color noise using a data acquisition system and calculating the power spectral density, this methodology is applied experimentally in three systems achieving to determine the color noise present.

**Color noise, Experimental process, Spectral slope**

#### Resumen

El objetivo principal de este trabajo es identificar los diferentes tipos de ruidos de color existentes en los sistemas eléctricos, se propone una metodología para la identificación de los ruidos de colores utilizando un sistema de adquisición de datos y calculando la densidad espectral de potencia, esta metodología se aplica de manera experimental en tres sistemas logrando determinar el ruido de color presente.

**Pendiente espectral, Análisis de Ruido, Ruido de colores**

**Citation:** HERNÁNDEZ-SANTIAGO, Joaquín, ALEJANDRO-CRISANTOS, Carlos, ESCOBEDO-TRUJILLO, Beatris Adriana, GARRIDO-MELÉNDEZ, Javier. Experimental analysis to identify colored noises in electrical systems. Journal of Systematic Innovation. 2022. 6-19: 31-41

\* Correspondence to Author (e-mail bescobedo@uv.mx:)

† Researcher contributing as first author.

## 1. Introduction

Noise is present in measurement systems and causes disturbances or fluctuations in the signals due to its random nature, Vasilescu (2005) mentions that the IEEE standard dictionary establishes and classifies noise by its origin: internally (from the system itself) and externally or interference (from another place and mixed with the signal of interest), both generate contamination in the signal and, to eliminate it, a filter is normally used, hence the importance of identifying the type of noise so that the proposed filter is adequate.

The work presented by Zhivomirov (2018) classifies noise into colours according to the behaviour of its spectral slope, also known as the power law, which is proportional to the reciprocal of the frequency  $f^\alpha$ . This is done by estimating the power spectral density.

The generation of coloured noise has been studied for a couple of decades, Corsini & Saletti (1988), Saletti (1986), Kasdin (1995) and Halford (1968) have provided different methods to create and analyse its behaviour. The modelling of an RC circuit with a current source with added white noise, which is used to generate other types of coloured noise and the analysis of pink noise are presented in the works of Keshner (1982) and Gruber (1986), finally, Murao *et al.* (1992) show the use of logarithmic and anti-logarithmic amplifiers for its generation.

There are applications of coloured noises: Pettai (1984) explains the different types of noises and their sources, including heat-generated noise. In the area of neuroscience, Galán (2009) applies low-amplitude colour noise for deep brain stimulation in order to control neuronal excitability efficiently. On the other hand, Bryson & Johansen (1965) reduce the amplitude of colour noise in dynamic systems using the Kalman filter.

In the electrical area there are several works, Ott (1988) makes an extensive study of noise in electronic systems: he determines its presence in passive elements, active noise devices and noise in digital circuits. Coloured noise is used by Mahdi (2018), which presents investigations of  $1/f$  noise fluctuations with different temperatures applied to a tunable laser diode configuration.

Also, Levinshtein & Romyantsev (2010) demonstrate the presence of  $1/f$  noise in different semiconductor devices and Nabati & Farnoosh (2021) have applied coloured noise generation in RLC-type circuits in a simulated manner. Most of the works described above only present the generation and simulation of coloured noises, without performing the experimental part of measurement and analysis. In this work, three systems are analysed (the sensor of a level control system, the current of a frequency converter and the voltage in the capacitor of an RLC circuit fed by a programmable voltage source) in order to detect and classify the types of colour noise present experimentally.

This work is divided in the following way, section 2 presents the methodology for the identification of the colour noise, section 3 shows the results obtained experimentally and section 4, the conclusions.

## 2. Methodology

### a. Colour noise classification

The classification of coloured noise depends on the power spectral density (PSD) of a measured signal and is determined by the following equation:

$$PSD \propto \frac{1}{f^\alpha} \quad (1)$$

Where  $f$  is the frequency in Hz and  $\alpha$  is an integer value bounded between -2 and 2, depending on the value of  $\alpha$  the noise is classified in the colours red, pink, white, blue and violet, each colour noise has different amplitudes depending on its frequency, these amplitudes increase or decrease, which can be plotted by a PSD where the slope shows the increase or decrease of decibels for each decade of frequency. Table 1 shows the properties of the above-mentioned coloured noises.

Noise Colour	Value of $\alpha$	Pending (dB/dec)
Red	Partition 1	-20
Pink	Partition 2	-10
White	Partition 3	0
Blue	Partition 4	10

**Table 1** Properties of coloured noises.

There are different ways to determine the PSD of a signal that is in the time domain, the one used in this work is the Welch averaged periodogram, defined as a non-parametric spectral estimator based on the classical periodogram that divides the signal spectrum into equal segments, develops a classical periodogram for each segment and determines an average of them.

The advantage of using the Welch averaged periodogram is that it allows overlap between segments, reduces the variance of the powers and maintains good resolution as a function of frequency. This is obtained using Matlab software and the methodology to determine it is as follows:

1. Divide the measured signal into equal segments (by default it is 8).
2. Perform the overlap or superimposition between segments (by default, 50% is considered).
3. For each segment, calculate the fast Fourier transform and square the magnitude to determine the power spectra.
4. Average the power spectra to obtain the averaged Welch periodogram.

Finally, the proposed methodology to determine the type of colour noise experimentally is:

1. Analyse the noise of the DAQ (Data Acquisitions System) system.
2. Measure the variables of the system, taking into account that the sampling frequency must be at least 100 times the highest frequency.
3. Calculate the PSD of the variable to be analysed considering the sampling frequency.
4. PSD analysis (the increment or decrement value in db/dec).
5. Classify the type of colour noise present.
  - a. Experimental systems

In this work, measurements on three systems are presented: the MPCT process control system, a variable frequency drive applied to a three-phase motor and a series RLC circuit fed with a programmable voltage source. A description of the electrical system as well as the data acquisition system is given in this section.

#### i. Process Control System (PPCS)

The MPCT shown in Figure 1 is a system that allows to control process variables such as: temperature, pressure, flow and level, the signal to be analysed is the voltage generated by the level sensor, which is a differential pressure sensor that produces a voltage proportional to the value of the level of the tank.



Figure 1 Process control system

The DAQ to be used is NI-Crio-9068 with the NI-9220 module, which is programmed using LabVIEW software in the FPGA and HOST interface, the level sensor signal is a dc signal proportional to the tank level, for the analysis a sampling frequency of 100 kHz was selected, the measured data are stored in a file in TDMS format, for subsequent analysis in the frequency domain in Matlab and display the PSD of the measured signal. Figure 2 shows the front panel of the HOST interface where the graph of the measured values in real time can be observed.

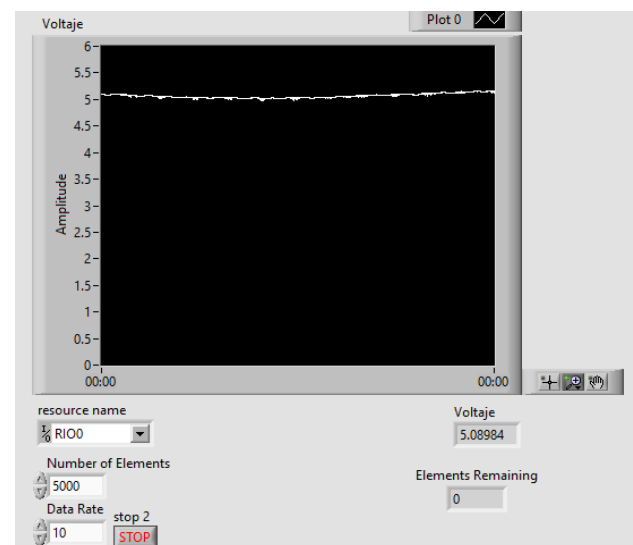


Figure 2 Host interface front panel

**i. Frequency inverter applied to a three-phase motor**



**Figure 3** Three-phase motor speed control system

A frequency inverter is a device for controlling the speed of electric motors. The equipment used is the "Micromaster 420 inverter", which is connected to a three-phase motor and its parameters are shown in Table 2. The signal to be analysed is the electric current, which contains noise produced by electronic components such as IGBTs. Figure 3 shows the frequency inverter, the motor used and the data acquisition system, which is the NI Crio-9068 connected to the NI 9246 readout card.

Variable	Value
Voltage	220 C
Current	1.8 A
Frequency	60 Hz
Power	1180 hp
Speed	1800 rpm

**Table 2** Three-phase motor parameters



**Figure 4** Wiring diagram used for noise analysis

The DAQ used is programmed in the two interfaces of the LabVIEW software, whose front panel of the Host is shown in Figure 5. The signals to be analysed are the currents of the three-phase motor, with three different frequencies 40, 50 and 60 Hz working at full load, for the analysis a sampling frequency of 50 kHz was selected.

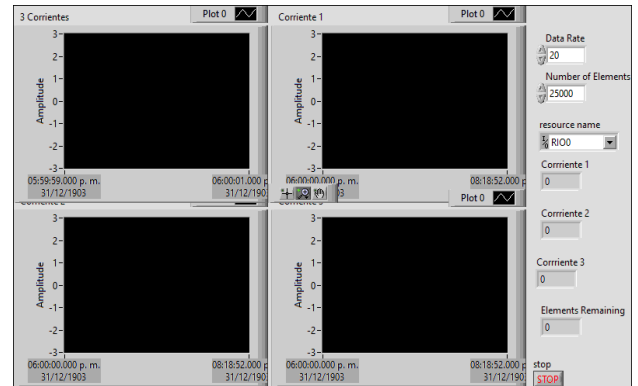


**Figure 5** Front panel for taking current readings

**i. Serial RLC circuit connected to a programmable power source**

The voltage source used is the "Programmable AC/DC Power Source APS-1102", this equipment provides voltages of up to 400 Vdc and 280 Vrms with output signals in DC, AC sinusoidal or square and with variable frequency. The purpose of using this equipment is to detect the type of colour noise generated by its electronic components, the physical connection of the data acquisition system connected to the serial RLC circuit is shown in Figure 6.



**Figure 6** Data acquisition system connected to the RLC circuit.

An RLC circuit is a second order linear system that is usually used as an analogue filter configured in a range of frequencies, it is formed by a resistor (R), an inductor (L) and a capacitor (C), the values selected for each element are in Table 3. The signal to be analysed is the voltage on the capacitor and the inductor current, in order to check the noise generated by the external power supply and the passive components of the circuit.

Variable	Value
Resistance (R)	546.23 Ω
Inductor (L)	1 H
Capacitor (C)	571.43 nF

**Table 3** RLC circuit elements

The series RLC circuit has the particularity of acting as a second order low-pass filter, allowing frequencies below the cut-off frequency  $f_c$  to pass through and attenuating those above it. The cut-off frequency is determined by the transfer function of the system and is given by equation (2), substituting the selected values for the RLC circuit we obtain a cut-off frequency of  $f_c = 210.5419 \text{ Hz}$ .

$$f_c = \frac{1}{2\pi\sqrt{LC}} \text{ Hz} \quad (2)$$

The DAQ to be used is a Crio 9068, with the 9246 and 9242 cards to measure current and voltage respectively, the voltage and frequency configurations to be analysed are presented in Table 4, for the analysis a sampling frequency of 50 kHz was established, the graphs of the measured data are presented in Figure 7.

No.	Waveform	Input voltage ( $V_{rms}$ )	Frequency (Hz)
1	Sine	200	50
2	Sine	200	60
3	Square	150	20
4	Square	250	180

Table 4 Programmable source configurations

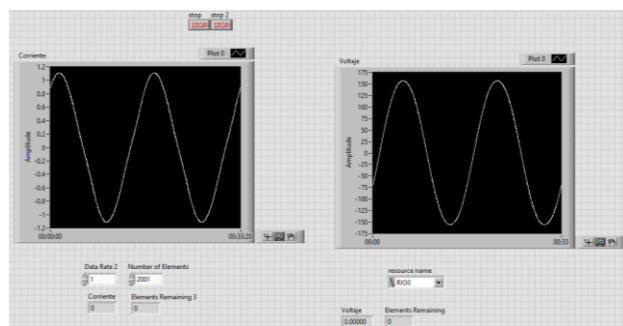


Figure 7 Host interface for taking current and voltage readings

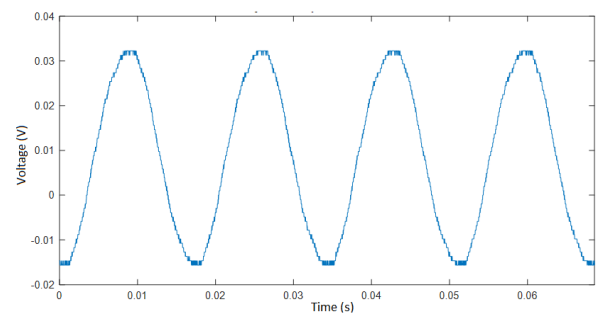
### 3. Results

The results of the measurements performed on the DAQ without connection to any system, the MPCT system, the variable frequency drive and the RLC circuit with a programmable voltage source are described. First a brief explanation of the time domain results is given and then their PSD is analysed to determine the noise colour based on their spectral slope and Table 2.

#### a. DAQ measurements

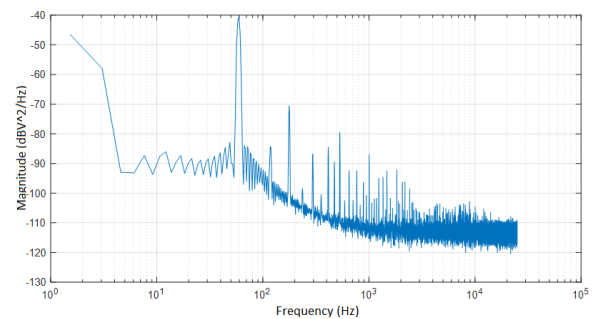
Figure 8 shows the measurements made to the NI-9220 module without connection, on the left shows the noise signal in the time domain, where you can see that has a sinusoidal shape with an amplitude ranging between -0.02 and 0.03, on the right is the PSD, which shows that the spectral slope is 0 value, therefore, the noise generated by the dc voltage reading module is white.

NI-9220 module in the CRio (50 kS/s)



(a)

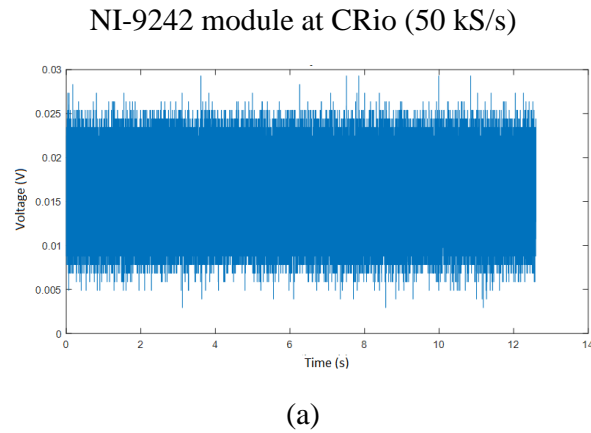
PSD of the NI-9220 Module in the CRio (50 kS/s)



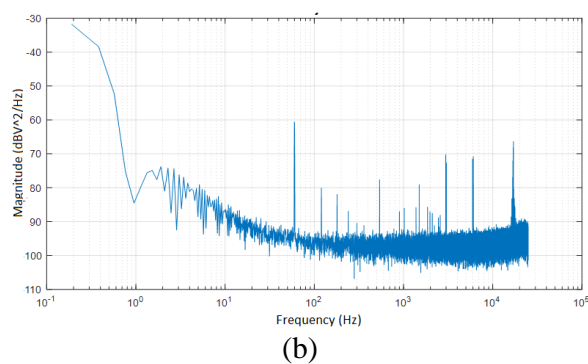
(b)

Figure 8 Measurement of the DAQ-9220

Figure 9 shows the measurement of the 9242 module without being connected to a system, in the time domain there is a lot of randomness of the measured signal, from the PSD it is observed that the power remains constant, which indicates that the noise produced is white.



PSD of the NI-9242 Module at the CRio (50 kS/s)



**Figure 9** Measurement of the DAQ-9242

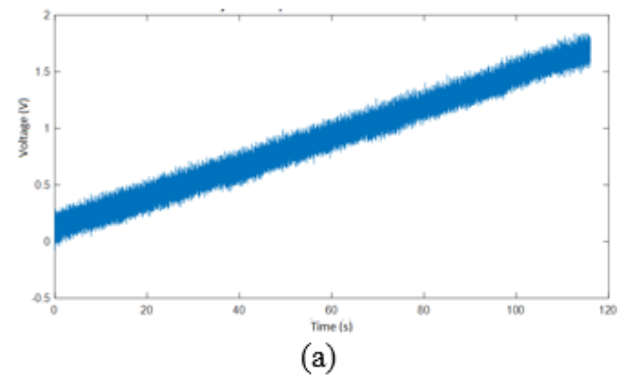
### b. Process Control System (MCPT)

The MPCT results are shown in two cases: the transient state, referred to the process where the water level is at 0 and rises until it reaches the reference level of the system and the steady state, given when the reference value has been reached and the water level does not vary, the reference value used for this system was 50 cm level.

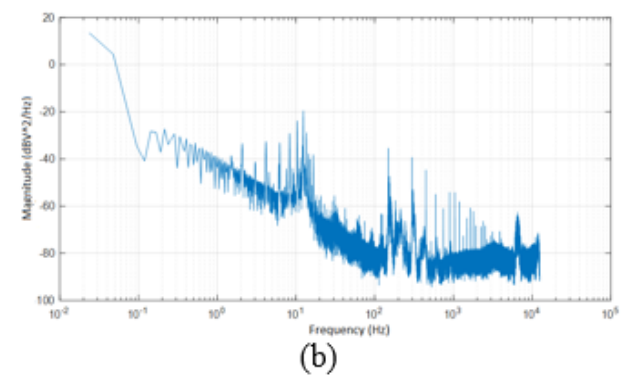
Figure 10 (a) shows the signal measured in transient state in the time domain sampled at a frequency of 25 kS/s for a time span of 70 s, it is observed that the tank level signal is very noisy, but it is not possible to classify the type of noise present, therefore, it is necessary to analyse it in the frequency domain.

Figure 10 (b) shows the MPCT measurement in transient state, where the PSD decreases by -20 db/dec (red noise) at low frequencies (up to 100 Hz), at high frequencies the PSD remains flat (white noise).

MPCT signal in transient state (25 kS/s)



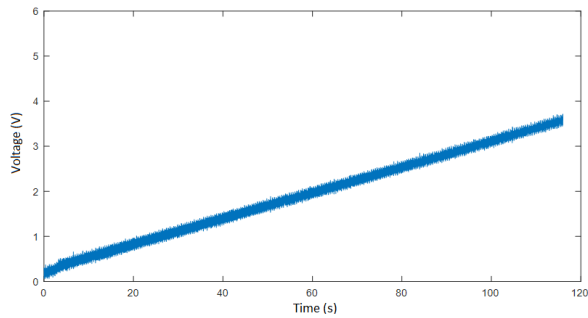
PSD of the signal measured in the MPCT



**Figure 10** MPCT in transient state (25 kS/s)

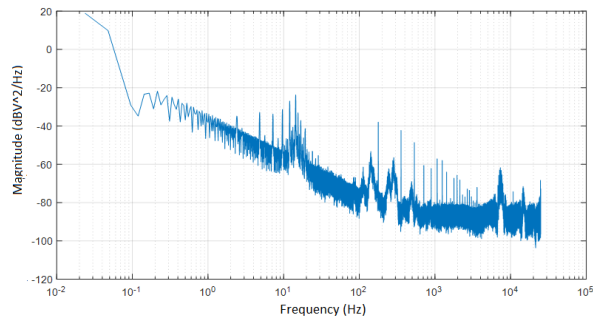
To demonstrate that the sampling frequency is independent of the noise present in the system, a sampling frequency of 50 kS/s was used. In the PSD of the signal measured at higher frequency is shown in Figure 11 (b), where it is observed that the spectral slope has a value of -20 db/dec, the colour noise present is red and as in Figure 10 (b), presents a white noise at high frequencies (slope value 0), therefore, it is concluded that the MPCT system in transient state presents a red noise regardless of the sampling frequency at which the DAQ is configured.

MPCT signal in transient state (50 kS/s)



(a)

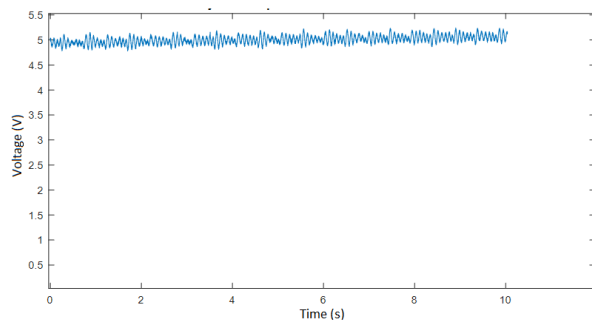
PSD of the signal measured in the MPCT



(b)

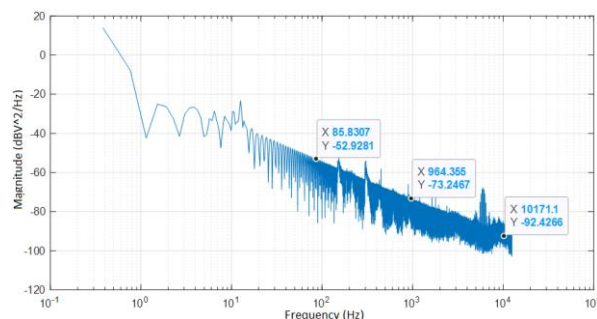
**Figure 11** MPCT in transient state (50 kS/s)

Steady state MPCT signal (25 kS/s)



(a)

PSD of the signal measured in the MPCT



(b)

**Figure 12** Steady-state MPCT (25 kS/s)

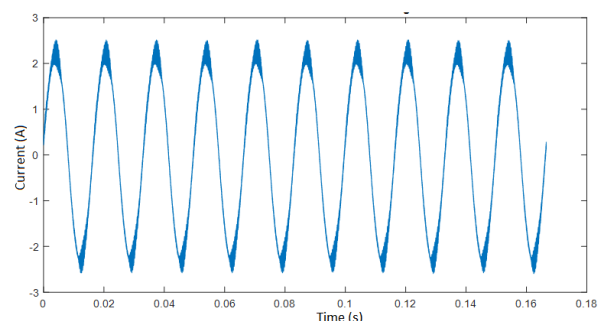
Figure 12 (a) shows the results of measuring the system in steady state at 25 kS/s, the measured value stays around 5V (proportional to the 50 cm level). Figure 12 (b) shows that the PSD has a slope that decreases by 20 db/dec, which is characteristic of red noise. Therefore, it is concluded that in steady state and transient the noise present in the system is red.

**c. Frequency inverter**

The analysis of the noise present in the frequency inverter is carried out by measuring the motor current, only the results of a single phase are shown because the three measured signals are the same.

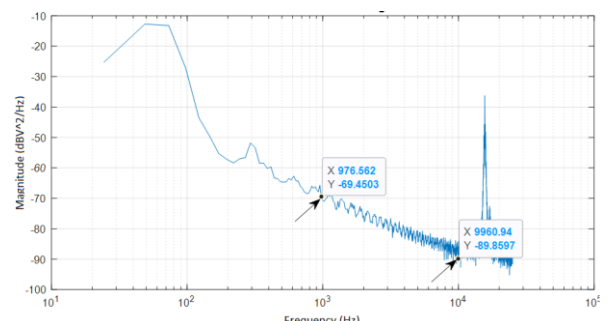
The tests carried out at the frequencies of 60, 50 and 40 Hz are shown in Figures 13 to 15 respectively, where the graphs at the top represent the signal in the time domain and the figures at the bottom are the PSD. It is observed the existence of noise in the current signal in the time domain, being more noticeable in the peak of the sine wave signal, however, this is not enough to classify the type of noise.

Signal in the time domain (60 Hz)



(a)

Spectral Power Density



(b)

**Figure 13** Single-phase measurements of motor current under load (set to 60 Hz)

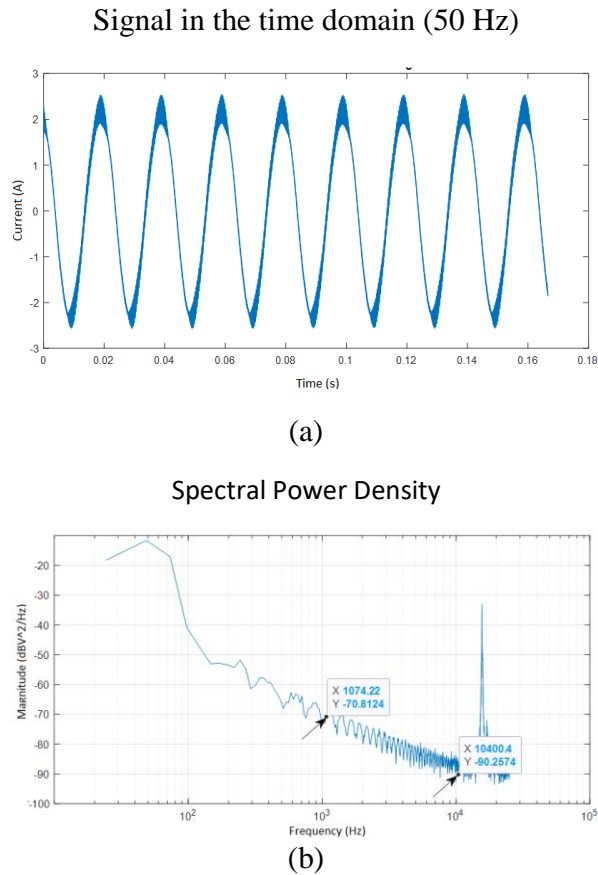


Figure 14 Single-phase measurements of motor current under load (set to 50 Hz)

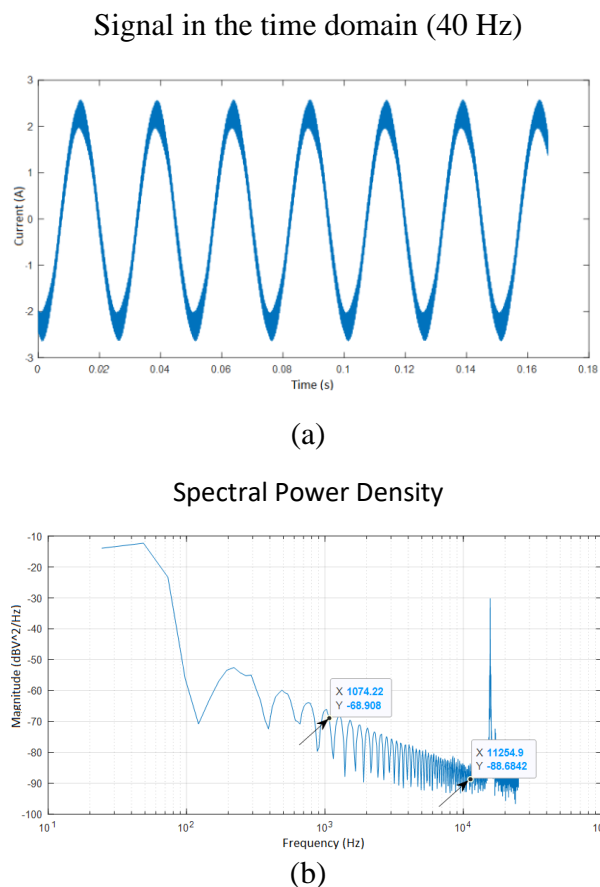


Figure 15 Single-phase measurements of the motor current under load (set at 40 Hz)

Analysing the signal in the frequency domain, it is observed that the power is reduced by 20 db/dec, this value is typical of the red noise. Therefore, after analysing the PSD of Figures 13 to 15, it can be concluded that, regardless of the operating frequency of the frequency inverter, the red noise is present.

**d. Serial RLC circuit connected to a programmable source**

In this section, the measurements made on the circuit with different input voltages, frequencies, and signals are analysed, as shown in Table 2. In the voltage and current signals obtained in the serial RLC circuit no noise is observed in the analysis in the time domain, however, the study of the same signals in the frequency domain is observed that, even when the amplitude is very low can be classified in a colour.

The results of measurement 1 are shown in Figures 16 and 17, where the signal voltage measured on the capacitor and the current of the RLC circuit are shown in the time domain, at the bottom of each Figure is its PSD. When analysing the spectral slopes, it can be seen that the noise presented by the external source signal is red, this is due to the fact that the noise power decays in 20 db/dec.

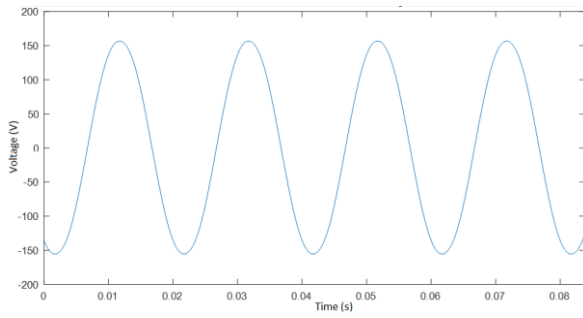
Figures 18 and 19 show the results of measurement 2, in this case, from the PSD the 60 Hz component associated to the input signal can be observed, in the same way as the first measurement, the noise present in the system is red, this is due to the fact that the PSD power is reduced by 20 db/dec.

The results of the third measurement are shown in Figures 20 and 21, in this case, the graphs in the time domain are slightly modified by the capacitive and inductive components, its load in the first half cycle and discharge in the second cause the signal measured and supplied by the voltage source are different, in the right column are observed the PSD corresponding to the voltage and current, they present a greater fluctuation, but the red noise can still be detected by the analysis of the spectral slope. Figures 22 and 23 show the graphs corresponding to the fourth measurement, unlike the previous case, the waveform is affected in the current, the PSD of voltage presents a decrease of 20 db/dec preserving the red noise colour, however, the PSD of current is reduced by 10 db/dec, value belonging to the pink noise.



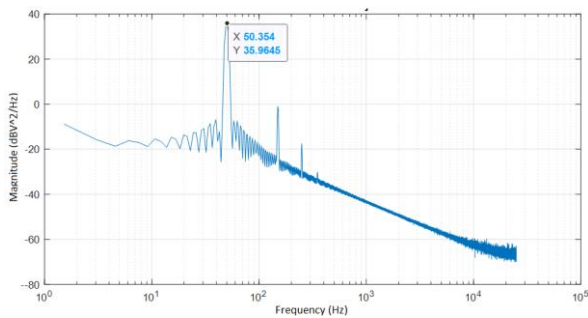
$$V_i = 200 V_{RMS}, \quad f = 50 \text{ Hz}$$

Time domain voltage



(a)

Spectral Power Density

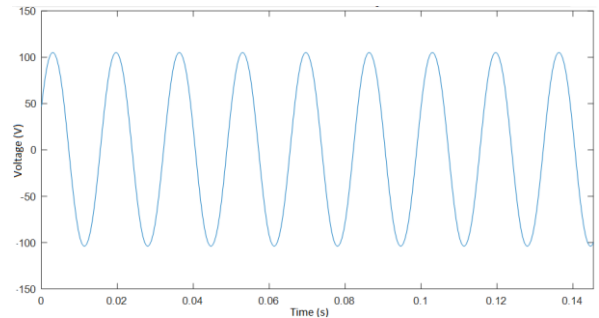


(b)

Figure 16 Capacitor voltage of the circuit fed with 200 Vrms at 50 Hz (sine wave signal)

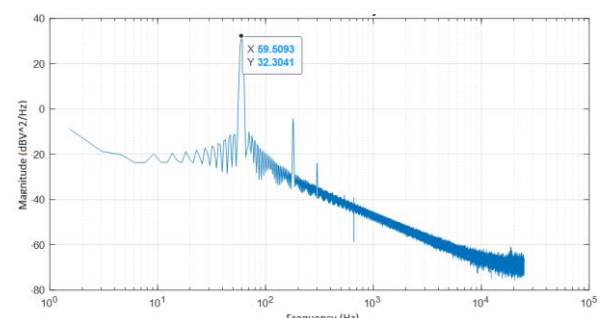
$$V_i = 200 V_{RMS}, \quad f = 60 \text{ Hz}$$

Time domain voltage



(a)

Spectral Power Density

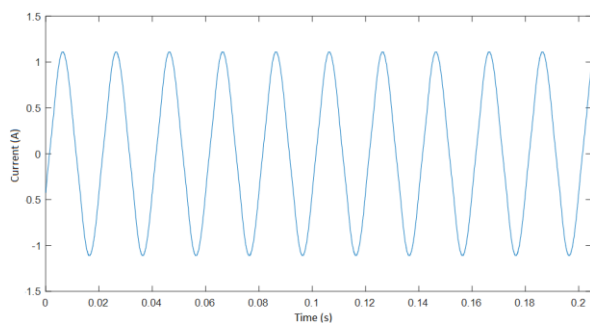


(b)

Figure 18 Capacitor voltage of the circuit fed with 200 Vrms at 60 Hz (sine wave signal)

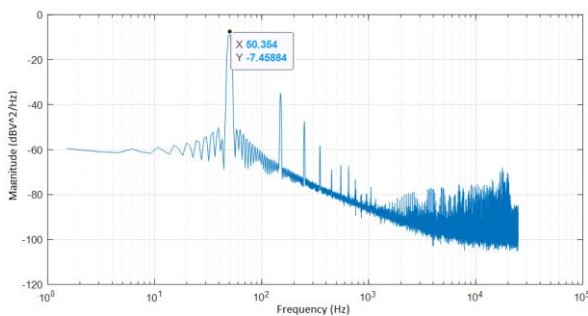
$$V_i = 200 V_{RMS}, \quad f = 50 \text{ Hz}$$

Corriente en el dominio del tiempo



(a)

Densidad Espectral de Potencia

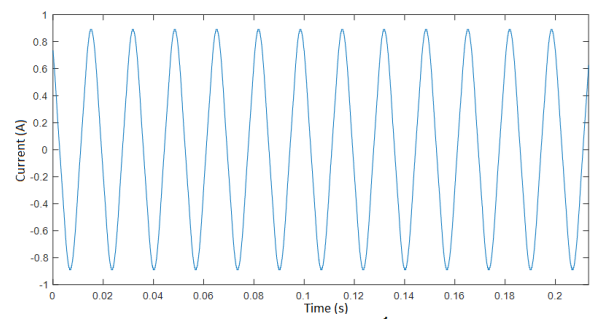


(b)

Figure 17 Current in the circuit fed with 200 Vrms at 50 Hz (sine-wave signal)

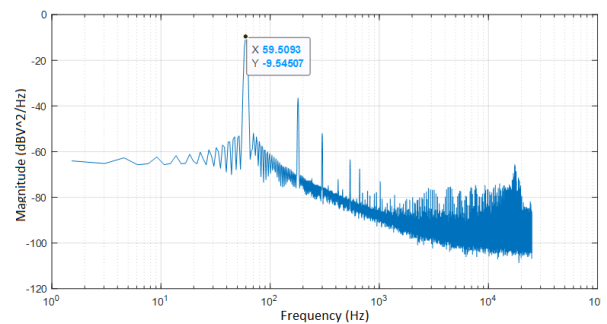
$$V_i = 200 V_{RMS}, \quad f = 60 \text{ Hz}$$

Time domain current



(a)

Spectral Power Density

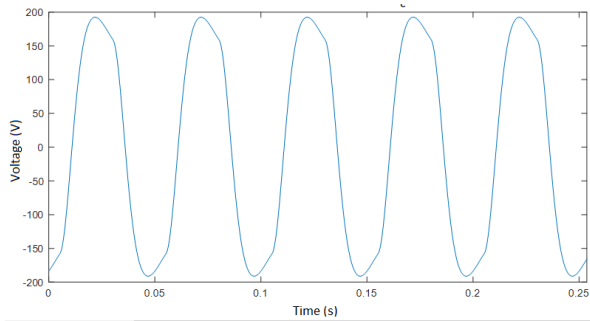


(b)

Figure 19 Current in the circuit fed with 200 Vrms at 60 Hz (sine-wave signal)

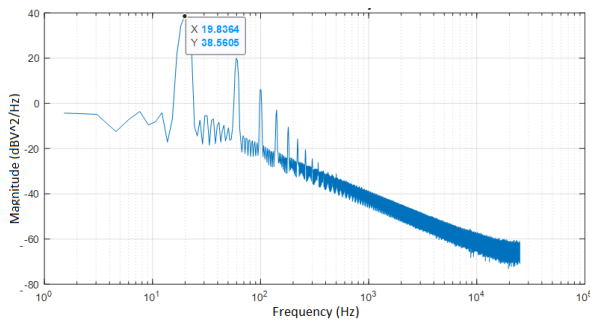
$$V_i = 150 V_{RMS}, \quad f = 20 \text{ Hz}$$

Time domain voltage



(a)

Spectral Power Density

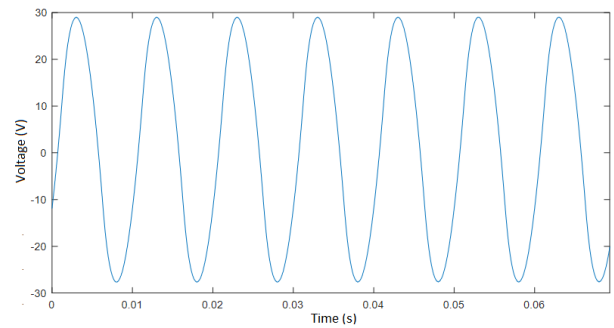


(b)

**Figure 20** Capacitor voltage of the circuit fed with 150 Vrms at 20 Hz (square signal)

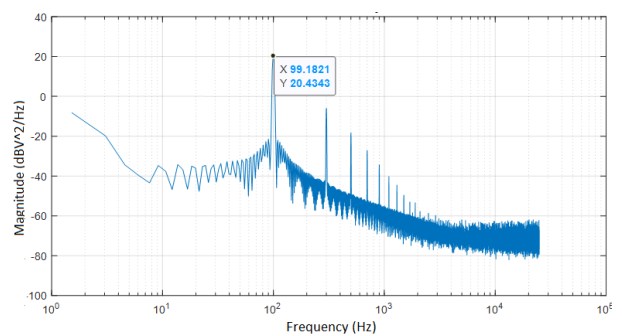
$$V_i = 200 V_{RMS}, \quad f = 100 \text{ Hz}$$

Time domain voltage



(a)

Spectral Power Density

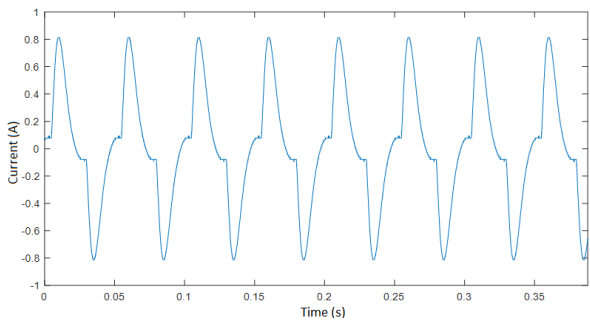


(b)

**Figure 22** Voltage at capacitor of circuit fed with 200 Vrms at 100 Hz (square signal)

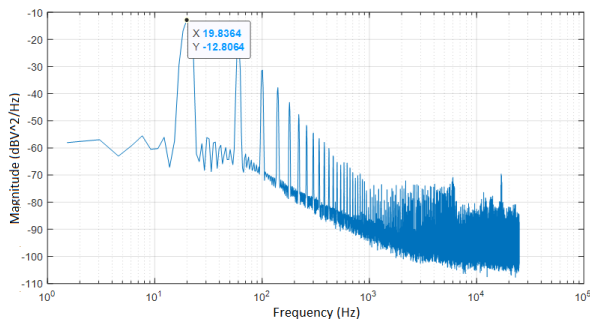
$$V_i = 150 V_{RMS}, \quad f = 20 \text{ Hz}$$

Time domain current



(a)

Spectral Power Density

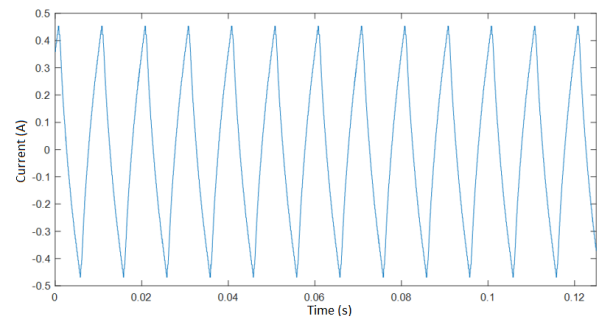


(b)

**Figure 21** Current in the circuit fed with 150 Vrms at 20 Hz (square signal)

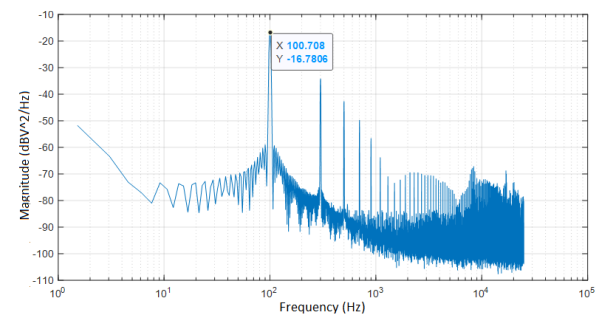
$$V_i = 200 V_{RMS}, \quad f = 100 \text{ Hz}$$

Time domain current



(a)

Spectral Power Density



(b)

**Figure 23** Current in the circuit fed with 200 Vrms at 100 Hz (square signal)

#### 4. Conclusions

After performing the measurements and analysing the power spectral density of the signals, it is concluded that the electrical systems contain noise (in greater or lesser quantity) and can be of different colours. To detect the type of colour noise it is not necessary to generate or simulate them, from the PSD it is possible to observe the increase or decrease of decibels per decade and from this, classify it into a colour. It is possible that some system generates a noise that is not appreciable in the time domain, the analysis of the PSD belonging to the frequency domain can detect the type of colour noise present in the system even when its amplitude is very small any electrical equipment has colour noise present, this could be verified in the three experimentally analysed systems.

#### 5. References

- Bryson, A., & Johansen, D. (1965). Linear filtering for time-varying systems using measurements containing colored noise. *IEEE Transactions on Automatic Control*, 10(1), 4–10. <https://doi.org/10.1109/TAC.1965.1098063>
- Corsini, G., & Saletti, R. (1988). A  $1/f^\gamma$  power spectrum noise sequence generator. *IEEE Transactions on Instrumentation and Measurement*, 37(4), 615–619. <https://doi.org/10.1109/19.9825>
- Galán, R. F. (2009). Frequency control in neuronal oscillators using colored noise. *BMC Neuroscience*, 10(Suppl 1), 252. <https://doi.org/10.1186/1471-2202-10-S1-P252>
- Gruber, P. (1986).  $1/f$ -NOISE GENERATOR. En *Noise in Physical Systems and  $1/f$  Noise 1985* (pp. 357–360). Elsevier. <https://doi.org/10.1016/B978-0-444-86992-0.50078-3>
- Halford, D. (1968). A general mechanical model for  $|f|^\alpha$  spectral density random noise with special reference to flicker noise  $1/|f|$ . *Proceedings of the IEEE*, 56(3), 251–258. <https://doi.org/10.1109/PROC.1968.6269>
- Kasdin, N. J. (1995). Discrete simulation of colored noise and stochastic processes and  $1/f$  power law noise generation. *Proceedings of the IEEE*, 83(5), 802–827. <https://doi.org/10.1109/5.381848>
- Keshner, M. S. (1982).  $1/f$  noise. *Proceedings of the IEEE*, 70(3), 212–218. <https://doi.org/10.1109/PROC.1982.12282>
- Levinshtein, M. E., & Romyantsev, S. L. (2010).  $1/f$  Noise: The Funeral is Cancelled (or Postponed). En *Future Trends in Microelectronics* (pp. 239–245). John Wiley & Sons, Inc. <https://doi.org/10.1002/9780470649343.ch20>
- Mahdi, S. A. (2018). The power spectral density of  $1/f$  noise in a tunable diode laser at different temperatures. *Journal of Optics*, 47(1), 61–64. <https://doi.org/10.1007/s12596-017-0426-x>
- Murao, K., Kohda, T., Noda, K., & Yanase, M. (1992).  $1/f$  noise generator using logarithmic and antilogarithmic amplifiers. *IEEE Transactions on Circuits and Systems I: Fundamental Theory and Applications*, 39(10), 851–853. <https://doi.org/10.1109/81.199872>
- Nabati, P., & Farnoosh, R. (2021). Stochastic approach for noise analysis and parameter estimation for RC and RLC electrical circuits. *International Journal of Nonlinear Analysis and Applications*, 12(1), 433–444.
- Ott, H. W. (1988). *Noise Reduction Techniques in Electronic Systems* (2a ed.). Wiley Interscience.
- Pettai, R. (1984). *Noise in Receiving Systems* (ilustrada). Wiley-Interscience.
- Saletti, R. (1986). A comparison between two methods to generate  $1/f^\gamma$  noise. *Proceedings of the IEEE*, 74(11), 1595–1596. <https://doi.org/10.1109/PROC.1986.13672>
- Vasilescu, G. (2005). *Electronic Noise and Interfering Signals* (1a ed.). Springer Berlin, Heidelberg.
- Zhivomirov, H. (2018). A Method for Colored Noise Generation. *Romanian Journal of Acoustics and Vibration*, 15(1), 14–19. <http://tjav.sra.ro/index.php/tjav/article/view/40>